Nanoscale

REVIEW

View Article Online
View Journal | View Issue

Cite this: *Nanoscale*, 2024, **16**, 3211

In situ peptide assemblies for bacterial infection imaging and treatment

Yanyan Zhou,†[a,b] Lingling Xu,†[c] Xianbao Sun,[c] Wenjun Zhan*[c] and Gaolin Liang *[c]

Received 2nd November 2023,
Accepted 13th January 2024

DOI: 10.1039/d3nr05557d

rsc.li/nanoscale

Bacterial infections, especially antibiotic-resistant ones, remain a major threat to human health. Advances in nanotechnology have led to the development of numerous antimicrobial nanomaterials. Among them, *in situ* peptide assemblies, formed by biomarker-triggered self-assembly of peptide-based building blocks, have received increasing attention due to their unique merits of good spatiotemporal controllability and excellent disease accumulation and retention. In recent years, a variety of "turn on" imaging probes and activatable antibacterial agents based on *in situ* peptide assemblies have been developed, providing promising alternatives for the treatment and diagnosis of bacterial infections. In this review, we introduce representative design strategies for *in situ* peptide assemblies and highlight the bacterial infection imaging and treatment applications of these supramolecular materials. Besides, current challenges in this field are proposed.

1. Introduction

Bacterial infection is the second leading cause of death worldwide and continues to threaten public health.[1] At present, antibiotic therapy remains the preferred first-line treatment option for bacterial infection patients. Unfortunately, treatment failure and relapse are increasingly common due to the emergence of notorious antibiotic resistance.[2–4] Twelve species of bacteria, including *Enterococcus faecium*, *Staphylococcus aureus* (*S. aureus*), *Klebsiella pneumoniae*, *Acinetobacter baumannii*, *Pseudomonas aeruginosa*, and *Enterobacter* (*i.e.*, ESKAPE pathogens), are listed as pathogens of particular concern by the World Health Organization.[5,6] To address the problem of resistance, high dose and frequent use of antibiotics are often required, which may in turn cause serious side effects.[7] Additionally, the number of antibiotic classes in the clinical pipeline is limited.[8] Thus, new antibacterial agents or regimens are in urgent demand.[9–15]

[a]*Collaborative Innovation Center of Advanced Microstructures, National Laboratory of Solid State Microstructure, Key Laboratory of Intelligent Optical Sensing and Manipulation, Ministry of Education, Department of Physics, Nanjing University, Nanjing 210093, China*
[b]*Wenzhou Key Laboratory of Biophysics, Wenzhou Institute, University of Chinese Academy of Sciences, Wenzhou, Zhejiang 325000, China*
[c]*State Key Laboratory of Digital Medical Engineering, School of Biological Science and Medical Engineering, Southeast University, 2 Sipailou, Nanjing, Jiangsu 210096, China. E-mail: wjzhan@seu.edu.cn, gliang@seu.edu.cn*
†These authors contributed equally to this work.

Yanyan Zhou

Yanyan Zhou received her B.S. degree from the Qingdao University of Science and Technology in 2013. She obtained her Ph.D. degree from Soochow University in 2019 under the supervision of Prof. Zhengbiao Zhang. She is currently working as a postdoctoral fellow at Nanjing University and the University of Chinese Academy of Sciences. Her research interests focus on molecular self-assembly and hydrogels.

Lingling Xu

Lingling Xu received her B.S. degree from Hubei Normal University in 2017. She obtained her M.S. degree from Zhengzhou University in 2020 under the supervision of Prof. Baoxian Ye. She is currently a Ph.D. candidate under the supervision of Prof. Gaolin Liang in the School of Biological Sciences and Medical Engineering at Southeast University. Her current research focuses on smart molecular probes, cellular imaging and biomedical analysis.

The rapid development of nanomaterials offers promising alternatives for antimicrobial therapy.[16,17] To date, numerous nanoantimicrobial agents have been developed, including metal nanoparticles,[18–20] carbon-based nanomaterials,[21,22] nanosized polymers,[23,24] upconverting nanoclusters,[25] hybrid nanomaterials,[26,27] and peptide assemblies.[28–33] Among them, peptide assemblies have attracted increasing attention due to their flexible design, easy synthesis, good biocompatibility, and excellent biodegradability.[34,35] In general, peptide assemblies refer to highly ordered nanostructures (*e.g.*, nanoparticles, nanofibers, nanotubes, *etc.*) formed by the molecular self-assembly of peptide-based building blocks.[36–39] Currently available peptide building blocks include aromatic peptides, lipopeptides, polypeptides, *etc.*[40–45] Traditional antimicrobial peptide assemblies are generally formed *in vitro* (*i.e.*, *ex situ* peptide assemblies). Recently, by rationally designing peptide precursors that respond to endogenous stimuli in a bacterial infection microenvironment (*e.g.*, pH, enzymes, and glutathione (GSH)), an "*in vivo* self-assembly" strategy was proposed for constructing peptide assemblies *in situ*.[46–49] Compared with *ex situ* peptide assemblies, these *in situ* assemblies exhibit improved spatiotemporal controllability, as well as enhanced disease accumulation and retention.[50] Therefore, excellent bacterial infection imaging and therapeutic outcomes can be easily achieved by covalently or physically introducing imaging probes/therapeutics into peptide precursors.[51,52] Remarkably, these *in situ* formed supramolecular materials can also interact with bacterial membranes or other cellular components, thereby conferring additional antibacterial activity on the assemblies. Taking advantage of these unique merits, we and other groups have explored antibacterial applications of *in situ* peptide assemblies. These advances urgently warrant a review on the progress made and the challenges ahead. Herein, in this review, we summarize the recent progress in *in situ* antibacterial peptide assemblies. First, molecular design strategies of peptide precursors (or monomers) are briefly introduced. Then, an overview of *in situ* peptide assemblies in bacterial infection imaging and treatment applications is provided. Finally, challenges and future directions in this field are discussed.

2. Molecular design principle

To achieve programmable and spatiotemporal control of *in situ* assemblies, great efforts have been devoted to the molecular design of peptide precursors (or monomers). By exploiting valuable stimuli in a bacterial infection microenvironment[53,54] (*e.g.*, pH, GSH, reactive oxygen species (ROS), enzymes, *etc.*), several strategies have been developed. Generally, *in situ* self-assembly strategies can be classified into four categories: cleavage-induced self-assembly, reaction-induced self-assembly, protonation/deprotonation-induced self-assembly, and target-induced self-assembly (Fig. 1). Cleavage-induced self-assembly is the most common type, in which peptide precursors directly transform into self-assembling monomers after enzymatic or chemical removal of a hydrophilic motif (Fig. 1a).[55] As for the reaction-induced self-assembly type, precursors undergo stimulus (or stimuli)-triggered chemical reactions (*e.g.*, condensation and polymerization) to yield their active monomers (Fig. 1b).[56] In contrast, peptide precursors in the protonation/deprotonation-induced self-assembly type do not undergo chemical bond cleavage or reaction to convert into self-assembling monomers, but instead rely on pH-triggered protonation or deprotonation (Fig. 1c).[57] While all of the three types above undergo stimulus-triggered conversion of precursors to monomers, the target-induced self-assembly type directly uses peptide monomers, whose *in situ* self-assembly is initiated by targeted accumulation in bacterial membranes or specific organelles (Fig. 1d).[58]

Xianbao Sun

Xianbao Sun received his BS degree from Anhui University in 2011. He obtained his PhD degree from the University of Science and Technology of China in 2019 under the supervision of Prof. Haojun Liang. He is currently working as a postdoctoral fellow in the School of Biological Sciences and Medical Engineering of Southeast University. His research interests focus on DNA nanotechnology, cellular imaging, and cancer diagnosis.

Wenjun Zhan

Wenjun Zhan received his B.S. degree from the Qingdao University of Science and Technology in 2013. He obtained his Ph.D. degree from Soochow University in 2018 under the supervision of Prof. Hong Chen and Prof. Qian Yu. During 2017–2018, he was a visiting student in Prof. Bing Xu's lab at Brandeis University. In 2019, he joined the School of Biological Sciences and Medical Engineering of Southeast University as an assistant professor. His current work focuses on the development of peptide hydrogels for applications in the biomedical and biotechnology fields.

3. *In situ* peptide assemblies for bacterial infection imaging

At present, clinical bacterial infection detection methods mainly include microbiological and biochemical analyses of blood, sputum, urine, stool, cerebrospinal fluid and other samples from patients.[59,60] However, these *in vitro* methods are often time-consuming and lack spatiotemporal accuracy.[61,62] To this end, developing molecular imaging probes for *in vivo* detection of bacterial infections is in urgent demand.[63] To date, different imaging modalities, including fluorescence (FL) imaging, photoacoustic (PA) imaging, and magnetic resonance (MR) imaging, have been developed by utilizing the concept of *in situ* peptide self-assembly. In this section, we focused on the application of *in situ* peptide assemblies in bacterial infection imaging in recent years.

3.1. Fluorescence imaging

FL imaging is considered as one of the most promising techniques for *in vivo* bacterial infection imaging due to its unique merits of superb sensitivity, high temporal resolution, fast-feedback, and non-ionizing radiation.[64] By conjugating organic small molecule dyes to self-assembling peptides, it is convenient to design fluorescent peptide probes with *in situ* self-assembly characteristics for bacterial infection imaging *in vivo*. As a typical example, Liu and co-workers synthesized a fluorescent peptide probe Rho-FF-Van consisting of a fluorescent dye rhodamine (Rho), a self-assembling dipeptide Phe-Phe (FF), and a Gram-positive bacteria targeting ligand vancomycin (Van).[65] *Via* the ligand–receptor interaction between Van and the D-Ala-D-Ala moiety in bacterial cell walls, Rho-FF-Van could specifically target Gram-positive bacteria (*e.g.* methicillin-resistant *staphylococcus aureus* (MRSA)) and further self-assembled into nanoaggregates on the bacterial membrane. Through the target-induced self-assembly process described above, the conjugated imaging motif Rho enriched at the infection site, leading to a significant increase in FL signal. Importantly, Rho-FF-Van could further be radiolabeled with iodine-125, enabling FL/nuclear-dual modal imaging in a mouse MRSA-pneumonia model. Nevertheless, traditional luminogens may suffer from the aggregation-caused quenching (ACQ) effect in the aggregate state, which may affect the imaging quality of this fluorescent peptide probe.

To address the above issues, FL probes with a "turn-on" feature were developed by covalently attaching aggregation-induced emission luminogens (AIEgens)[66,67] to biomarker-responsive peptides. For example, Liu *et al.* reported an AIEgen–peptide conjugate, PyTPE–CRP, for imaging intracellular bacterial infection *in vivo*.[68] The rationally designed peptide probe PyTPE–CRP contains a caspase-1-cleavable peptide NEAYVHDAP and an AIEgen PyTPE (Fig. 2a). After PyTPE–CRP was cleaved by caspase-1 (an upregulated enzyme during intracellular bacterial infection), its resultant residues self-assembled into nanoparticles *in situ*, thereby efficiently turning on the FL signal (Fig. 2b and c). The ability of PyTPE–CRP to detect intracellular bacteria *in vivo* was further verified using a mouse subcutaneous infection model. Specifically, *S. aureus*-infected Raw 264.7 cells or normal Raw 264.7 cells were subcutaneously injected into the mouse right flank, followed by intravenous injection of PyTPE–CRP. While mice treated with Raw 264.7 cells (control group) showed a negligible FL signal, mice treated with *S. aureus*-infected Raw 264.7 cells exhibited a bright FL signal at the infection site (Fig. 2d). Similarly, by conjugating AIEgens to self-assembling phosphopeptides, Yang and co-workers developed a series of peptide probes with *in situ* self-assembly properties for imaging ALP activity in living *Escherichia coli* (*E. coli*) cells.[69,70] Interestingly, the ALP detection ability of AIEgen–peptide conjugate probes could be well regulated by controlling the number of ALP-responsive sites (*i.e.*, phosphotyrosine) and self-assembling units (*i.e.*, phenylalanine), as well as the distance between the AIEgen and self-assembling phosphopeptide. The *in vivo* FL imaging performance of the above probes can be further enhanced by incorporating bacterial targeting ligands into the probe design.

3.2. Photoacoustic imaging

Newly emerging PA imaging has received increasing attention for accurate disease diagnosis because of its high spatial resolution, real-time visualization, and considerable tissue penetration.[71–73] To date, various well-established contrast agents, including inorganic materials,[74] small organic molecules[75] and semiconducting polymers[76] have been developed for PA imaging. However, these conventional contrast agents may self-aggregate or interact nonspecifically with biomolecules, which greatly affects their imaging quality or biosafety *in vivo*. Fortunately, the *in situ* assembly strategy provides a straightforward solution to resolve the above problem. In a typical study, Wang and co-workers synthesized a novel peptide-based contrast agent Mannose-Tyr-Val-His-Asp-Cys-

Gaolin Liang

Gaolin Liang is a full professor at Southeast University (SEU). He received his BS degree from Nanjing University in 1993 and his PhD degree from Fudan University in 2005. He was a postdoctoral fellow with Prof. Bing Xu at Hong Kong University of Science and Technology (2005–2008) and with Prof. Jianghong Rao at Stanford University (2008–2010). Then, he held a full professor position at the University of Science and Technology of China (from 2010 to 2021). He set up a group at SEU in 2018. His laboratory at SEU focuses on nanochemistry, molecular and cellular imaging, and biomedical analysis.

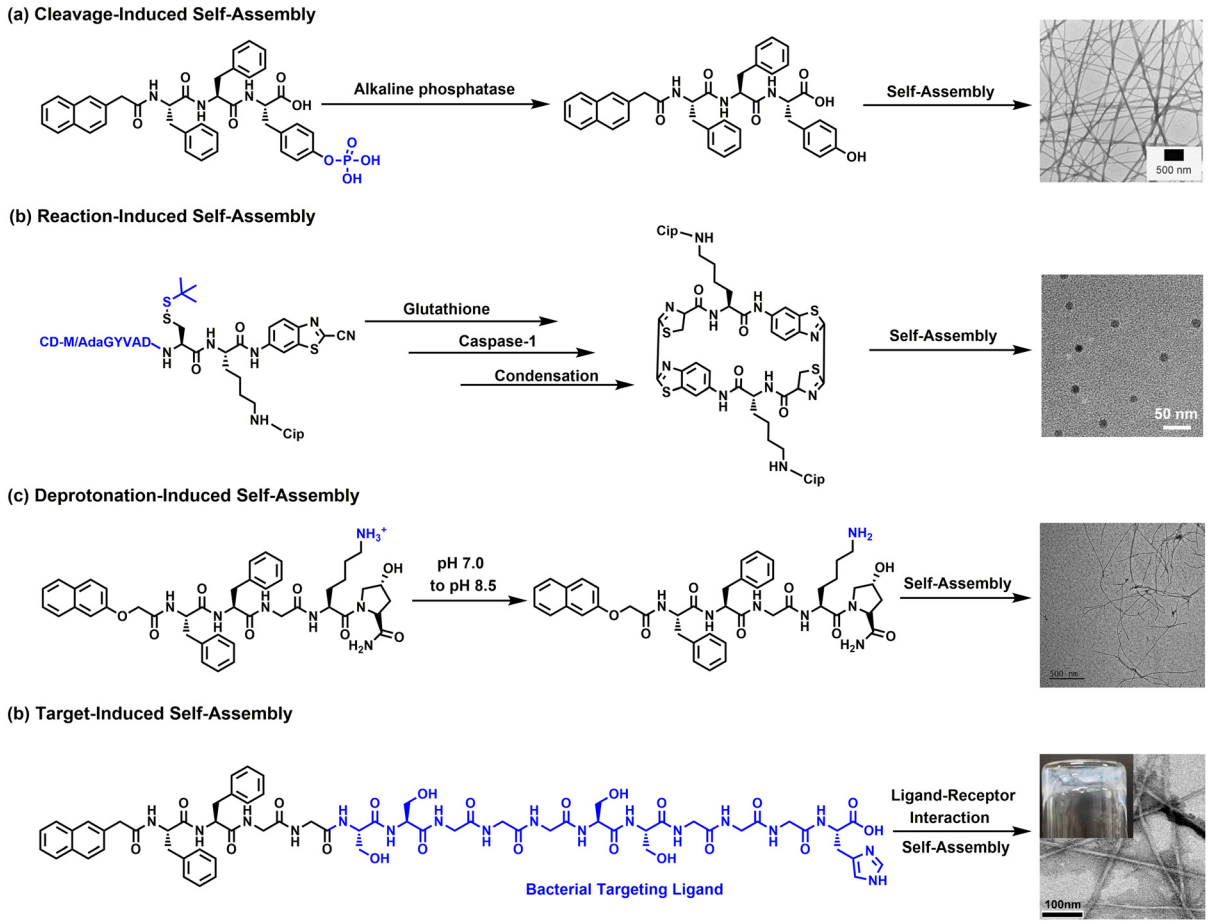

Fig. 1 (a) Representative example of cleavage-induced self-assembly. ALP removes a hydrophilic phosphate group from a phosphotripeptide precursor to trigger its *in situ* self-assembly. Reproduced with permission.[55] Copyright 2007, Wiley-VCH GmbH. (b) Representative example of reaction-induced self-assembly. GSH and caspase-1 initiate an intermolecular CBT-Cys condensation reaction between two Cip-CBT-Ada/CD-M precursors, yielding a cyclic dimer monomer that further self-assembles to form nanoparticles. Reproduced with permission.[56] Copyright 2023, Wiley-VCH GmbH. (c) Representative example of protonation/deprotonation-induced self-assembly. Deprotonation of a pentapeptide precursor converts it into an active monomer, which self-assembles into nanofibers. Reproduced with permission.[57] Copyright 2022, American Chemical Society. (d) Representative example of target-induced self-assembly. Ligand–receptor interaction guides the self-assembly of a bacterial targeting ligand-containing peptide monomer. Reproduced with permission.[58] Copyright 2023, American Chemical Society.

Lys-(Ala-P_{18}) (MPC), which consists of a macrophage-targeting motif mannose, a pentapeptide Tyr-Val-His-Asp-Cys (YVHDC) for caspase-1 tailoring, and an organic contrast agent purpurin 18 (P_{18}) (Fig. 3a).[77] Upon coordination with Cu^{2+}, MPC turned into dimers in water and actively targeted *S. aureus*-infected macrophages through specific recognition of membrane mannose receptors. After uptake, the MPC dimer was subjected to caspase-1 tailoring to yield P_RC, which further self-assembled into *J*-type aggregates inside infected macrophages (Fig. 3b). Consequently, the contrast agent P_{18} accumulated at the bacterial infection site due to the assembly-induced-retention (AIR) effect. Moreover, the self-assembly of P_RC could additionally induce PA signal enhancement. By constructing a mouse subcutaneous infection model, the authors further verified the ability of this MPC probe for enhanced PA imaging of intracellular infection *in vivo* (Fig. 3c). Specifically, the PA imaging signal of MPC at the infected site was 2.6-fold higher than that of the non-infected site (Fig. 3d). In a related work, the authors reported another peptide-based PA imaging probe, P18-YVHDC-TAT, for quantitative detection of caspase-1 activity in infected macrophages.[78] In addition to caspase-1, gelatinase overexpressed in a variety of bacteria (*e.g.*, *S. aureus*, *Staphylococcus epidermidis*, and *Proteus vulgaris*), has also been reported as a valuable stimulus for designing enzyme-activatable PA imaging probes.[79] These works provide powerful and noninvasive tools for real-time and quantitative analysis of bacterial infection *in vivo*.

This *in situ* self-assembly strategy can also be utilized to induce *in situ* aggregation of inorganic contrast agents to achieve enhanced PA imaging. For instance, Wang and coworkers designed a gold nanoparticle–peptide conjugate AuNPs@P1 by covalently modifying a functional peptide CLVFFAEDPLGVRGRVRSAPSSS (P1) on gold nanoparticles (AuNPs, a typical inorganic PA contrast agent).[80] The func-

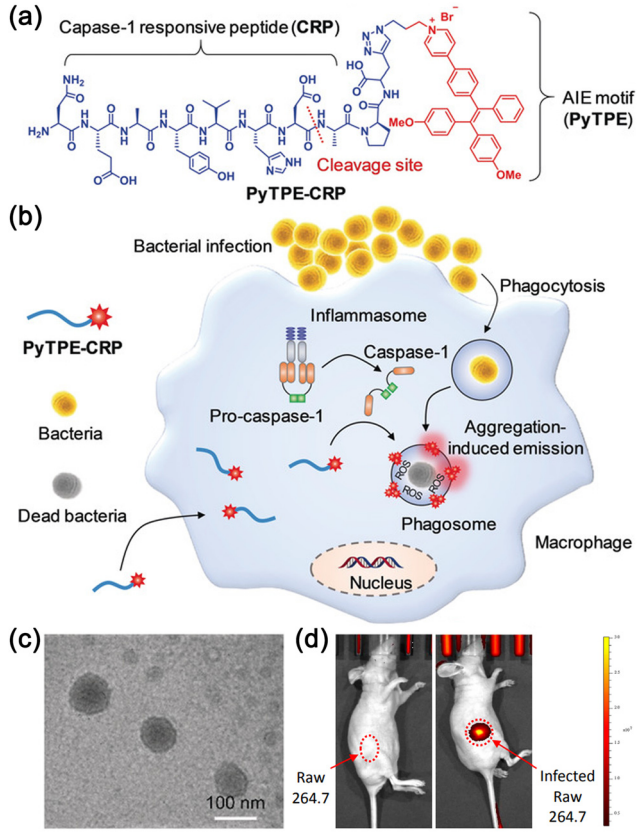

Fig. 2 (a) Chemical structure of PyTPE–CRP. (b) Schematic of macrophage-mediated intracellular bacterial infection diagnosis and elimination. (c) TEM image of PyTPE–CRP after treatment with activated caspase-1 enzyme. (d) *In vivo* fluorescence images of intracellular bacterium-bearing mice after intravenous (i.v.) injection of PyTPE–CRP. The Raw 264.7 cell- and *S. aureus* infected Raw 264.7 cell-treated regions are labeled with red dot circles. Reproduced with permission.[68] Copyright 2019, Wiley-VCH GmbH.

tional peptide P1 consists of three major parts: a self-assembling scaffold CLVFFAED, a collagenase IV (an overexpressed enzyme by *S. aureus*)-responsive linker PLGVRG, and a *S. aureus*-targeting ligand RVRSAPSSS. After administration, AuNPs@P1 could specifically bind to the *S. aureus* membrane at the infection site through an active targeting mechanism. Then, overexpressed collagenase IV selectively tailed conjugated P1 between G/V sites, triggering the self-assembly of AuNPs *in situ*. According to the authors, the as-formed aggregated AuNPs showed significant PA signal enhancement because of their increased heat conversion efficiency, as well as their enhanced retention and accumulation. By using this *in situ* self-assembly strategy, it will also be feasible to improve PA imaging efficiency of other types of contrast agents (*e.g.*, semiconducting polymers).

3.3. Magnetic resonance imaging

Although FL imaging and PA imaging are valuable for detecting superficial bacterial infections, their application in diagnosing deep bacterial infections is most unlikely. Alternatively, MR imaging offers a powerful method to resolve the above-mentioned problem due to its non-invasiveness, excellent soft tissue contrast, unlimited tissue penetration, high spatial resolution, and radiation-free features.[81] To achieve significant tissue contrast in infectious sites, molecular MR imaging based on different contrast agents was developed.[82] In particular, it has been reported that gadolinium (Gd)-based contrast agents capable of forming self-assemblies *in situ* can achieve enhanced MR imaging of pathological analytes.[83] In 2021, Song and co-workers developed a MR imaging probe GFV, which contains a bacterial target ligand Van, a T_1 contrast agent Gd^{3+}, and a self-assembling peptide FFYEGK.[84] On the one hand, the ligand Van enabled the probe to target *S. aureus* at the infection site. On the other hand, the self-assembling motif triggered the probe to form nanoaggregates, leading to enhanced T_1-weighted MR imaging of *S. aureus* infection *in vivo* at a low magnetic field of 0.5 T. Recently, Qiao and co-workers proposed a precise MR imaging-guided sonodynamic therapy based on smart polymer–peptide–porphyrin conjugate-1 (PPPC-1) to treat deep bacterial infection.[85] PPPC-1 is rationally designed to contain four parts: a hydrophobic polymer core bis-MPA polyester-64-hydroxyl, a self-assembling peptide linked with hydrophilic poly(ethylene glycol) (PEG) *via* a gelatinase-cleavable peptide (CGGGKLVFFPLGVRG-PEG2000), a *S. aureus*-targeting peptide CGGGTGRAKRRMQYNRR, and a manganese (Mn)-based contrast agent MnTCPP. PPPC-1 self-assembled in water to form nanoparticles (*i.e.*, PPPC-1 nanoparticles), which can actively target *S. aureus* and then turn into nanofibers after gelatinase cuts off the protecting PEG layers (Fig. 4a). The authors found that PPPC-1 nanoparticles before and after gelatinase activation showed basically consistent T_1-weighted signals (left column of Fig. 4b) and T_2-weighted signals (left column of Fig. 4c). In addition, linear relationships between the values of the longitudinal relaxation rate ($1/T_1$) or the transverse relaxation rate ($1/T_2$) and the Mn concentrations were observed (right column of Fig. 4b and c). By calculating the slope of the fitted linear curve, they found that PPPC-1 exhibited a high relaxivity r_1 of 6.65 mM^{-1} s^{-1} at 7 T (right column of Fig. 4b). Interestingly, this T_1-contrast agent-based PPPC-1 also showed a high relaxivity r_2 of 138.96 mM^{-1} s^{-1} (right column of Fig. 4c). The above findings provided a basis for monitoring the PPPC-1 concentration *in vivo* using T_1–T_2 dual-modal MR imaging. This assumption was validated in deep MRSA-infected mice treated with PBS, MnTCPP, PPPC-2 (morphology-unchanging control), and PPPC-1. As shown in Fig. 4d, the PPPC-1 group showed the most obvious T_1 and T_2 signals among the four groups. By using the formulas shown in Fig. 4b and c, the concentrations of PPPC-1 and PPPC-2 could be accurately quantified by T_1 combined T_2 (Fig. 4e). Therefore, precise MR imaging-guided sonodynamic therapy can be achieved using this smart PPPC-1 contrast agent. By utilizing other valuable stimuli in an infection microenvironment (*e.g.*, matrix metallopeptidase-2[86] and acid microenvironment[87]), more activatable MR imaging probes can be developed for precise bacterial infection imaging *in vivo*.

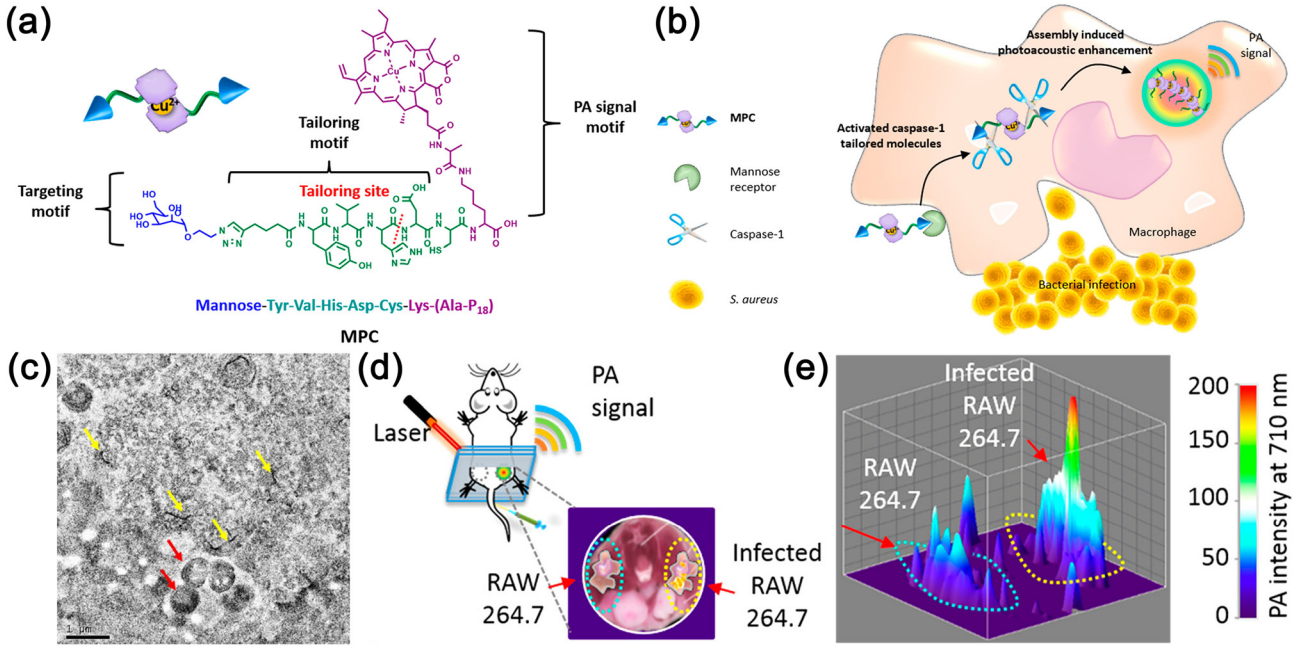

Fig. 3 (a) Molecular component of the probe (MPC). (b) Schematic representation of macrophage chemotaxis-instructed *S. aureus* infection detection *in vivo*. (c) The *in situ* characterization of intracellular construction of assembled structures (yellow arrows) in infectious cells. The *S. aureus* (red arrows) infected RAW 264.7 cells after treatment with MPC. The ultrathin sections of RAW 264.7 cells were stained by osmic acid and uranyl acetate before TEM studies. (d) Schematic illustration of the mouse model (intramuscular injection of infected RAW 264.7 cells) and photoacoustic tomography (PAT) detection. (e) PA signal intensity distribution of infected RAW 264.7 cells *in vivo* after MPC administration with a dose of 35 mg kg^{-1} though i.v. injection for 8 h. Reproduced with permission.[77] Copyright 2018, American Chemical Society.

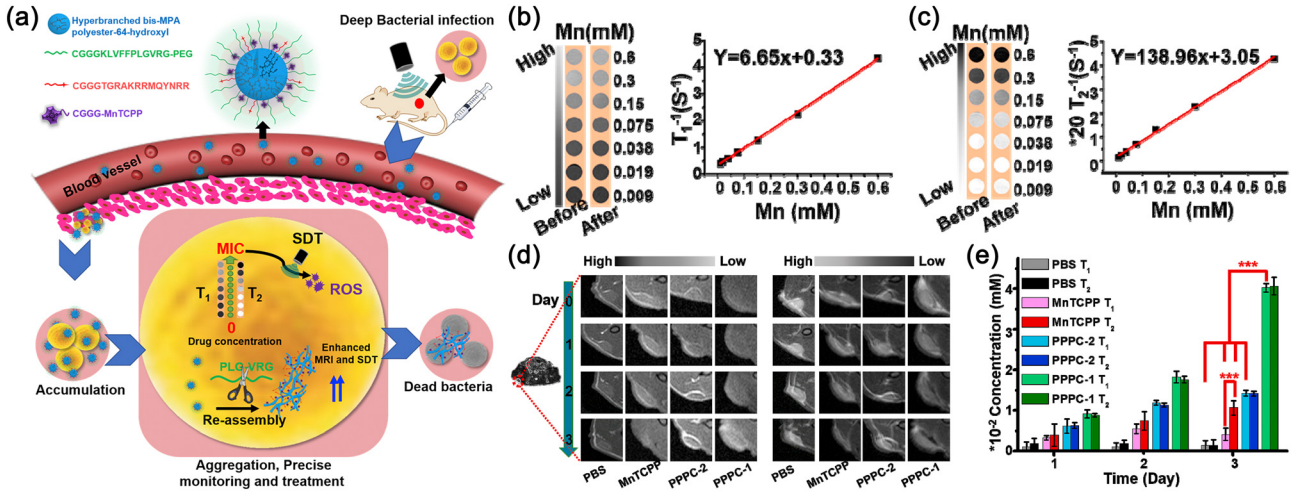

Fig. 4 (a) Schematic illustration of enzyme-induced morphology transformation of PPPC for precise magnetic resonance imaging-guided treatment of drug-resistant bacterial deep infection. (b) Left: T_1-weighted positive MRI signal of PPPC-1 before and after secondary assembly at different concentrations. Right: corresponding $\Delta 1/T_1$ *versus* Mn concentration in PPPC-1 buffer solutions measured by MRI. (c) Left: T_2-weighted positive MRI signal of PPPC-1 before and after secondary assembly at different concentrations. Right: corresponding $\Delta 1/T_2$ *versus* Mn concentration in PPPC-1 buffer solutions measured by MRI. (d) Representative MRI T_1 (left) and T_2 (right) contrasts at a bacterial infection site (red circle) in mice injected with PBS, MnTCPP, PPPC-2, and PPPC-1 for 3 days. (e) The calculated material concentration at the infection site. Reproduced with permission.[85] Copyright 2021, Elsevier Ltd.

4. *In situ* peptide assemblies for bacterial infection treatment

Pioneered by the Xu[88] and Ulijn[89] groups, *in situ* peptide self-assembly is envisaged to be a powerful method to control cell behaviors. In 2007, Xu and co-workers first reported the use of ALP to trigger the self-assembly and hydrogelation of synthetic peptides inside *E. coli* to inhibit its growth.[55] Since then, various *in situ* peptide assemblies with different antibacterial mechanisms has been developed, which will be discussed in the following section.

4.1. Drug delivery

Antibiotics have saved countless human lives since penicillin was first discovered in 1928. Nevertheless, their intrinsic limitations, including low specificity, severe off-target toxicity, and drug resistance, lead to increasing cases of treatment failure and relapse. To resolve the abovementioned issues, various antibiotic delivery strategies have been developed.[90–92] One promising strategy is to covalently attach antibiotics to *in situ* self-assembling peptides, as the resulting antibiotic–peptide conjugates display unique advantages of precise targeting, prolonged retention, and controlled antibiotic release at the infection sites.[56] Recently, by rationally designing a ciprofloxacin–peptide conjugate Cip-CBT-Ada, Liang and co-workers reported a smart strategy of tandem guest–host–receptor recognition to combat intracellular *S. aureus* infection. Specifically, Cip-CBT-Ada consists of the following parts: (1) an antibiotic ciprofloxacin; (2) a CBT motif; (3) a cysteine residue, whose thiol and amino are protected by the StBu group (substrate for GSH reduction) and Tyr-Val-Ala-Asp (substrate for Casp-1 cleavage), respectively; (4) a guest motif adamantane (Ada) (Fig. 5a). Cip-CBT-Ada could recognize β-cyclodextrin-heptamannoside (CD-M) *via* host–guest interaction to form a supramolecule Cip-CBT-Ada/CD-M. The formed Cip-CBT-Ada/CD-M could specifically target macrophages through multivalent ligand–receptor interaction between CD-M and mannose receptors on the macrophage membrane. Under the action of GSH and caspase-1, Cip-CBT-Ada/CD-M underwent a CBT-Cys condensation reaction to yield a cyclic dimer Cip-dimer, which further self-assembled into *in situ* ciprofloxacin nanoparticles. Through this, an antibiotic depot was formed inside *S. aureus*-infected macrophages, enabling long-term and sustained release of ciprofloxacin. As a result, Cip-CBT-Ada/CD-M showed enhanced *S. aureus* infection curing ability in a mouse subcutaneous model, as evidenced by immunofluorescence staining of pro-inflammatory cytokines (Fig. 5b) as well as plate colony counting of residual bacteria in infected tissues (Fig. 5c). Taken together, this work illustrates an intelligent manner to guide antibiotics to remove intracellular *S. aureus* effectively. In addition to covalent grafting, drugs can also be physically mixed with *in situ* self-assembling peptides to achieve accurate delivery. For example, Roy and co-workers developed a collagen-inspired peptide that spontaneously formed spherical nanoparticles for the encapsulation of ferulic acid.[57] Under the activation of a basic chronic wound environment, the drug-loaded nanoparticles underwent deprotonation-induced nanofiber transformation, accompanied by the release of ferulic acid. Such structural transformation of the peptide offers an efficient drug delivery strategy for treating bacterial infection and other diseases.

In situ self-assembling peptides can also be used to deliver non-antibiotic antibacterial agents. For instance, Liu *et al.* developed an AIEgen–peptide conjugate E-probe consisting of an AIEgen, a self-assembling peptide backbone, and a bacterial targeting ligand Van.[93] The Van motif can guide the E-probe to specifically target the D-Ala-D-Ala sequence on Gram-positive bacteria and trigger the formation of *in situ* aggregates through target-instructed self-assembly. As such, the probe turned the FL signal on and enhanced its ROS generation ability, thereby achieving efficient bacterial detection and photodynamic therapy in a mouse myositis model. In another recent work, Wan and co-workers used an acidic microenvironment (pH 4.5–6.5) to induce the charge reversal and self-aggregation of silver nanoparticles (Ag NPs) in bacterial biofilms.[94] In detail, Ag NPs–peptide and Ag NPs–CBT conjugates were prepared by grafting an undecapeptide NH_2-Lys-Arg_4-Gly-His_4-Cys-CM and CBT to small Ag NPs, respectively. Under physiological conditions, the grafted undecapeptide could fold through intramolecular hydrogen bonding, leaving its cysteine protected. After the Ag NPs–peptide conjugate reached the bacterial infection tissues with an acidic microenvironment, its histidine imidazole groups became protonated, converting surface charge to positive to efficiently target the negatively charged bacterial cell wall. In addition, the Ag NP–peptide conjugate exposed its 1,2-thiol amino group to initiate a CBT-Cys condensation reaction between the Ag NPs–CBT conjugate, resulting in the *in situ* formation of clustered Ag NPs. Consequently, enhanced accumulation and retention of Ag NPs in biofilms were achieved, leading to efficient bacterial biofilm disruption both *in vitro* and *in vivo*. The above antibiotic-free *in situ* self-assemblies may provide promising alternatives to overcome antibiotic resistance.[95,96]

4.2. Bacterial membrane disruption

In situ self-assemblies can also directly kill bacteria through rational design. A common strategy is to introduce positively charged groups into a peptide precursor. In a typical work, Qiao *et al.* reported a chitosan–peptide conjugate (CPC) composed of a chitosan backbone, a gelatinase-responsive motif GPLGVRGC, a hydrophilic PEG, and a positively charged peptide sequence CGGGKLAKLAKKLAKLAK (KLAK).[97] After its PEG motif was tailored by overexpressed gelatinase at the infectious site, the CPC underwent a nanoparticle-to-nanofiber transformation *in situ*. Consequently, the formed nanofiber assemblies exposed their positively charged KLAK motifs to disrupt the negatively charged bacterial membrane through multivalent cooperative electrostatic interactions. Importantly, the above-mentioned *in situ* morphological transformation process also significantly promoted the accumulation and retention of CPC at bacterial infection sites, leading to

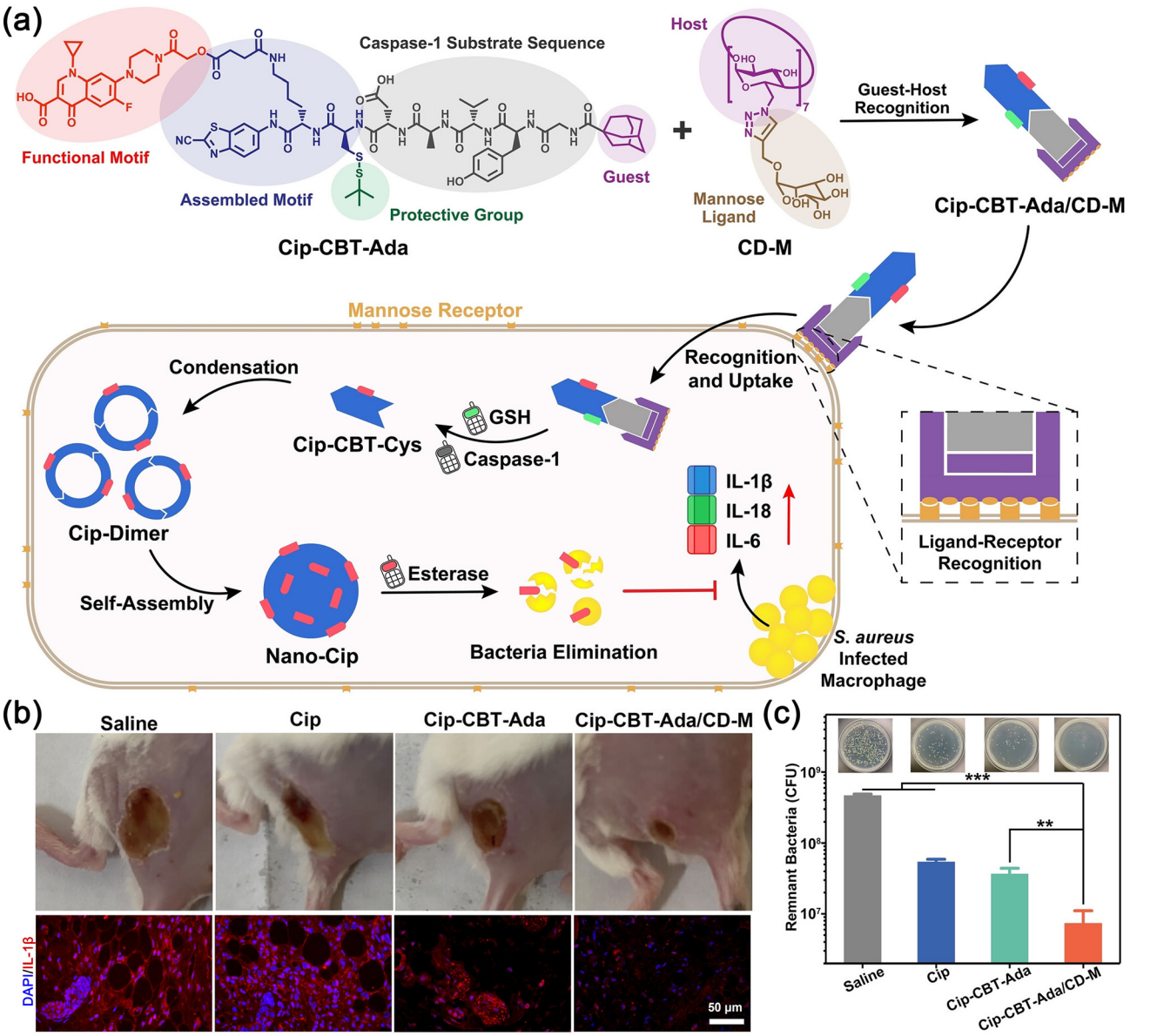

Fig. 5 (a) Schematic illustration of the strategy of tandem guest–host-receptor recognition to precisely guide ciprofloxacin to eliminate intracellular *S. aureus*. (b) Top: representative photos of *S. aureus*-infected mice at day 3 after different treatments. Bottom: immunofluorescence staining of IL-1β in infected tissues at day 3. (c) Representative photos and quantification of *S. aureus* colonies harvested from infected tissues at day 3. Reproduced with permission.[56] Copyright 2023, Wiley-VCH GmbH.

enhanced antibacterial efficacy *in vivo*. Similarly, the authors used gelatinase to trigger a wound dressing to release a peptide monomer containing a $(KLAKLAK)_2$ sequence.[98] The released peptide monomer subsequently self-assembled into fibrous nanostructures *in situ*, enabling efficient sterilization in wound infections. In another recent work, Du *et al.* developed a peptide precursor WRWRWY consisting of three hydrophobic tryptophans (W), two arginines (R) with positively charged side chains, and a tyrosine for tyrosinase (an overexpressed enzyme in the human skin) oxidation.[99] Upon tyrosinase activation, WRWRWY self-assembled into *in situ* mWRWRWY nanoparticles, whose surface exposed multivalent positive charges to disrupt bacterial membranes. Furthermore, tyrosinase oxidation could generate melanin-like moieties in the assemblies, thereby scavenging free radicals in infected wounds. Such a synergistic effect could efficiently promote wound healing. Other oxidases, like plasma amine oxidase (PAO), were also reported to induce peptide precursors to form *in situ* antimicrobial assemblies.[100]

Besides enzymes, the acidic microenvironment can also serve as a valuable stimulus to trigger the formation of positively charged assemblies at the infection sites. For example, Qin and co-workers constructed a charge-reversible lipopeptide C_{16}-A_3K_4(DMA)-$CONH_2$, in which ε-amino groups of lysine were protected by negatively charged dimethylmaleic amide (DMA).[101] C_{16}-A_3K_4(DMA)-$CONH_2$ formed a nanosphere struc-

ture under physiological conditions. After the C_{16}-A_3K_4(DMA)-$CONH_2$ nanoparticles reached the acidic microbial infection site, their ε-amino groups were deprotected, exposing the positively charged $-NH_3^+$. Meanwhile, the C_{16}-A_3K_4(DMA)-$CONH_2$ nanoparticles transformed into C_{16}-A_3K_4-$CONH_2$ nanorods, which facilitated their binding with bacterial membranes. Through this, the antibacterial activity of the lipopeptide was efficiently switched on. Recently, Ma and co-workers developed a chimeric peptide containing a self-assembling motif C_{14} alkyl chain, a pH-responsive and β-sheet domain $(HHHF)_4$, a hydrophilic PEG sequence, and a *P. aeruginosa*-targeting ligand QRKLAAKLT.[102] Remarkably, the acidic environment led to the protonation of histidine residues, triggering the nanofiber-to-nanofiber transformation of the chimeric peptide. As a result, the chimeric peptide reduced its size to efficiently penetrate bacterial biofilms, as well as turned on its positive charge to kill drug-resistant *P. aeruginosa*. Apart from the acidic microenvironment, the negatively charged lipid membrane also emerged as a potential trigger for the generation of *in situ* assemblies that disrupt bacterial membranes.[103]

Hydrogels are considered as promising candidates for wound healing treatments due to their extracellular matrix–mimicking feature.[104–106] Taking this into consideration, Liang and co-workers developed Nap-FYp-Ada, an adamantane–peptide conjugate precursor that enzymatically self-assembled into *in situ* nanofibers and hydrogels to kill *S. aureus*.[107] Specifically, Nap-FYp-Ada comprised a self-assembling peptide motif Nap-Phe-Phe (Nap-FF), a phosphatase substrate phosphotyrosine (Yp), and an Ada group (Fig. 6a). Under ALP cleavage, Nap-FYp-Ada evolved into the monomer form Nap-FY-Ada, which self-assembled into Nap-FY-Ada nanofibers on cytoplasmic lipids of *S. aureus* and subsequently caused bacterial membrane disruption (Fig. 6a). An *in vitro* experiment showed that a transparent and stable hydrogel formed after adding ALP to Nap-FYp-Ada solution (Fig. 6b). While Nap-FYp-Ada exhibited a wound healing rate of over 90% on day 7, its non-self-assembling control (*i.e.*, Nap-AYp-Ada) and adamantane-blocking control (*i.e.*, Nap-FYp-Ada/CD) showed much weaker ability to promote wound healing (Fig. 6c). In addition, Nap-FYp-Ada killed *S. aureus* cells at wound sites efficiently (>95%) (Fig. 6d). Different from cationic peptide precursors,

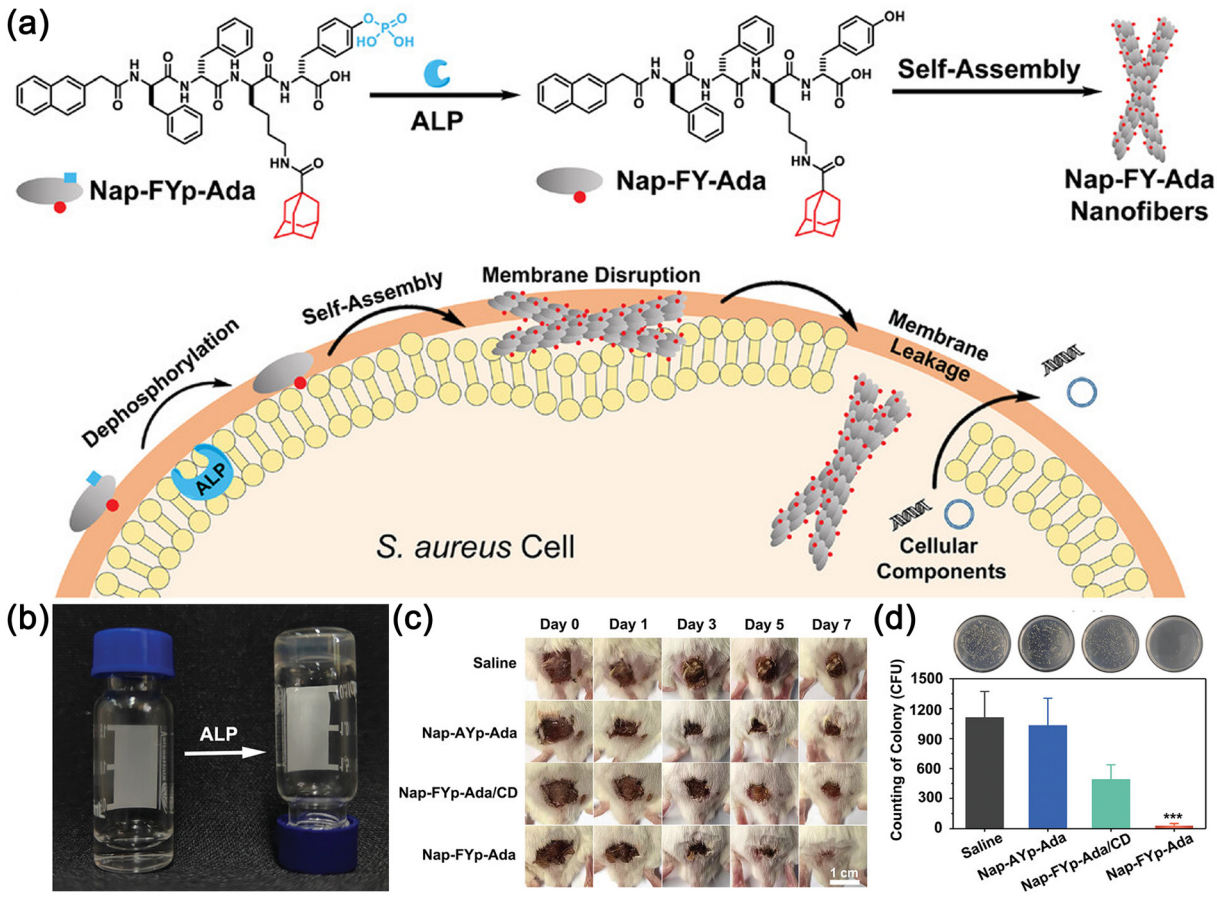

Fig. 6 (a) Top: chemical structure of Nap-FYp-Ada and the schematic of its enzymatic transformation. Bottom: cartoon illustration of the antimicrobial mechanism of Nap-FYp-Ada *via in situ* enzymatic self-assembly. (b) Photographs of 0.5 wt% Nap-FYp-Ada before and after incubation with 20 U mL^{-1} ALP at 37 °C for 18 h. (c) Representative photographs of the *S. aureus*-infected mice taken at day 0, 1, 3, 5, and 7 after different treatments. (d) Representative photographs of *S. aureus* cultures on LB–agar plates from infected-tissues at day 7 and the corresponding statistics of *S. aureus* colonies. Reproduced with permission.[107] Copyright 2023, Wiley-VCH GmbH.

this adamantane–peptide precursor relies on an adamantane motif (rather than positively charged groups) to interact with bacterial cells, thus providing an alternative strategy for the design of antimicrobial peptides.

4.3. Bacteria trapping

When encountering invading bacteria, some endogenous antimicrobial peptides (*e.g.*, human defensin-6 (HD6)) do not kill them directly, but self-assemble to form entangled fibrous networks to trap them and prevent their invasion.[108] From a biomimetic point of view, it is thus of considerable interest to develop *in situ* peptide assemblies with the bacteria trapping capability. In a representative study, Wang and co-workers reported an HD-6 mimic peptide (HDMP) that efficiently recognizes and captures bacteria *in vivo*.[109] The HDMP bis-pyrene-KLVFF-RLYLRIGRR is rationally designed to contain three components: (1) a particulate unit bis-pyrene; (2) a self-assembling unit KLVFF that derived from β-amyloid; (3) a recognition unit RLYLRIGRR, which serves as a ligand to bind with lipoteichoic acid (LTA) of Gram-positive bacteria (Fig. 7a). HDMP first

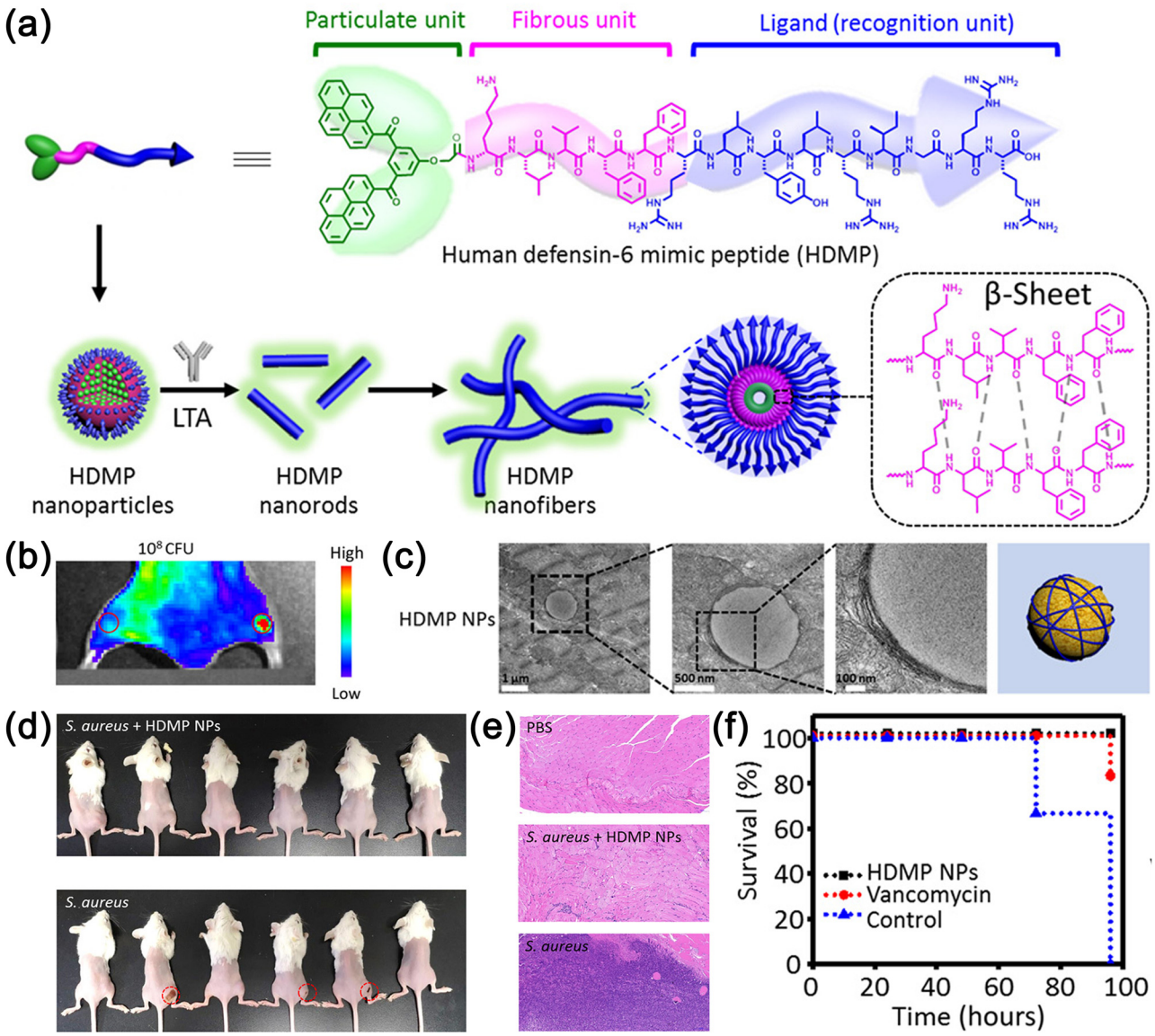

Fig. 7 (a) Molecular structure of HDMP and schematic illustration of HDMP assembly into NPs, transforming into nanorods and nanofibers (NFs) upon the incubation of lipoteichoic acid (LTA). (b) *In vivo* fluorescence images of leg muscle inoculated with 10^8 CFU bacteria (right) and PBS (left), followed by HDMP NP intravenous administration. (c) The TEM images of muscle tissue slices inoculated with *S. aureus* and treated with HDMP, showing transformed HDMP NFs on bacterial surfaces. (d) Images of *S. aureus* inoculated in the right leg muscles in mice in the presence and absence of HDMP NPs. (e) The representative hematoxylin and eosin (H&E) staining images of the leg muscle tissue of mice, indicating that the HDMP NP-treated *S. aureus* did not induce the bacterial infection. (f) Survival curve of the bacteremia mice infected by methicillin-resistant *S. aureus* (MRSA) treated with HDMP NPs, compared with vancomycin. Reproduced with permission.[109] Copyright 2020, American Association for the Advancement of Science.

self-assembled into nanoparticles (HDMP NPs) in water. After specific binding to LTA of Gram-positive bacteria (*e.g.*, *S. aureus*) through ligand–receptor interaction, HDMP NPs could transform into *in situ* nanofibers (HDMP NFs) with a β-sheet secondary structure (Fig. 7a). To verify the bacteria trapping of HDMP *in vivo*, the authors constructed a mouse muscle infection model. Specifically, the leg muscles of each mouse were inoculated with PBS (left) and 10^8 CFU *S. aureus* (right), respectively, followed by intravenous injection of HDMP NPs. As expected, only the right leg muscle (*i.e.*, the bacteria infection site) showed a bright pyrene FL signal, suggesting that HDMP NPs could target *S. aureus in vivo* (Fig. 7b). Meanwhile, obvious fibrous networks were observed around *S. aureus* surfaces in infection tissues, indicating that HDMP NPs underwent ligand–receptor-triggered morphological transformation *in vivo* (Fig. 7c). Next, the authors assessed the antibacterial activity of HDMP NPs *in vivo* using a mouse abscess model. As shown in Fig. 7d, while all mice in the "*S. aureus* + HDMP NPs" group showed no obvious infection, three out of six mice in the "*S. aureus*" group exhibited apparent abscess infection. Furthermore, hematoxylin and eosin (H&E) staining revealed a significantly reduced number of inflammatory cells in the leg muscle tissue of the "*S. aureus* + HDMP NPs" group, confirming that HDMP NPs could effectively suppress *S. aureus* invasion *in vivo* (Fig. 7e). Additionally, they validated the effectiveness of HDMP NPs in the treatment of MRSA bacteremia, as evidenced by the improved survival of bacteremic mice received HDMP NP treatment (Fig. 7f). In another related study, Shi and co-workers synthesized a peptide N-K10 by conjugating a clumping factor B (ClfB, a receptor protein expressed on the *S. aureus* cell wall)-targeting ligand SSGGGSSGGGH to the self-assembling motif Nap-FF *via* a diglycine linker.[58] According to the authors, N-K10 could specifically recognize ClfB-rich bacteria (*i.e.*, *S. aureus* and MRSA) and further self-assemble into nanofibers to trap the bacteria. As such, the invasion ability of ClfB-rich bacteria was efficiently inhibited. These works provide a novel "trap but not kill" strategy for the design of antimicrobial agents.

Besides target-induced self-assembly, other *in situ* self-assembly strategies were also reported to design bacterium trapping peptides. In a recent work, Gao and co-workers exploited upregulated ROS to induce the formation *in situ*

Table 1 Summary of *in situ* peptide assemblies for bacterial infection imaging and treatment applications

Peptide sequence	Stimulus	Assembly	Application	Ref
Rho-FFYEGK(Van)	D-Ala-D-Ala	Nanoaggregate	FL	65
NEAYNEAP-PyTPE	Caspase-1	Nanoparticle	FL	68
TPEPy-^{D}F^{D}FpY^{D}EG^{D}K	ALP	Nanofiber	FL	69
TPE-fffpYpYEEE	ALP	Nanoparticle	FL	70
Mannose-YVHDCK(AP18)	Caspase-1	Nanofiber	PA	77
P18-YVHDC-TAT	Caspase-1	Nanoaggregate	PA	78
Ppa-PLGVRG-Van	Gelatinase	Nanofiber	PA	79
AuNPs@CLVFFAEDPLGVRGRVRSAPSSS	Collagenase IV	Aggregated AuNPs	PA	80
Gd-FFYEGK-Van	D-Ala-D-Ala	Nanoparticle	MRI	84
Polymer-CGGG-KLVFFPLGVRG-PEG/TGRAKRRMQYNRR/MnTCPP	Gelatinase	Nanoparticle	MRI	85
Ada-GYVADC(StBu)K(Cip)-CBT	GSH, Caspase-1	Nanoparticle	Drug delivery	56
NapFFGKO	pH	Nanoparticle-to-nanofiber	Drug delivery	57
TPE-^{D}F^{D}F^{D}Y^{D}EG^{D}K(Van)	D-Ala-D-Ala	Nanoaggregate	Drug delivery	93
Ag NPs-KR_4GH_4C(CM), Ag NPs-CBT	pH	Aggregated Ag NPs	Drug delivery	94
Chitosan-GPLGVRGCPEG/CGGGKLAKLAKKLAKLAK	Gelatinase	Nanoparticle-to-nanofiber	Membrane disruption	97
SF-GAGAGSGPLGVRGLVFF$(KLAKLAK)_2$	Gelatinase	Nanofiber	Membrane disruption	98
WRWRWY	Tyrosinase	Nanoparticle	Membrane disruption	99
Ac-VVVVVVKKK	PAO	Nanoparticle-to-nanofiber	Membrane disruption	100
C_{16}-A_3K_4(DMA)-$CONH_2$	pH	Nanoparticle-to-nanorod	Membrane disruption	101
C_{14}-$(HHHF)_4$-K(PEG_8)-QRKLAAKLT	pH	Nanofiber-to-nanofiber	Membrane disruption	102
KRRFFRRK	Bacterial membrane	Nanofiber	Membrane disruption	103
NapFFK(Ada)Yp	ALP	Nanofiber	Membrane disruption	107
Bispyrene-KLVFF-RLYLRIGRR	Lipoteichoic acid	Nanoparticle-to-nanofiber	Bacteria trapping	109
Nap-FF-GG-SSGGGSSGGGH	Clumping factor B	Nanofiber	Bacteria trapping	58
BQA-GGFF	ROS	Nanofiber	Bacteria trapping	110
NQ-FF	Nitroreductase	Nanofiber	Bacteria trapping	111
C_{16}-LVFFA-KKRAKKFFKKPRVIGVSIPF, C_{16}-LVFFA-$(SG)_5$	Membrane components	Nanoparticle-to-nanofiber	Bacteria trapping	112

peptide assemblies to prevent bacterial invasion.[110] In detail, they designed a peptide precursor BQA-GGFF composed of a ROS-activatable fluorogenic motif (BOA) and a self-assembling motif GGFF. Upon the action of an inflammatory microenvironment, BQA-GGFF evolved into its monomer form BQH-GGFF and further self-assembled into fluorescent nanofibers at bacterial infection sites. The *in situ* formed nanofibrous networks not only served as artificial neutrophil extracellular traps (NETs) to inhibit bacterial dissemination, but also acted as a ROS scavenger to reduce inflammation levels. Therefore, a smart negative feedback system was created to efficiently fight bacterial infections. In another important work, they developed a peptide-based precursor NQF containing a nitroreductase (NTR, an enzyme overexpressed by *Fusobacterium nucleatum*)-responsive quinazolinone core (NQ) and the self-assembling motif FF.[111] Upon NTR activation, NQF converted into its monomer form HQF, which self-assembled into *in situ* nanofibers to trap *Fusobacterium nucleatum*, leading to bacterial membrane damage and growth inhibition. Notably, the authors found that the antibacterial assemblies could further promote chemotherapy for colorectal cancer, a malignancy associated with *Fusobacterium nucleatum*. Recently, Li and co-workers reported a multifunctional peptide system with antibiotic loading, bacterial membrane disruption, and bacterium-trapping properties for the treatment of multidrug resistant bacterial pneumonia.[112] Specifically, a cathelicidin-based lipopeptide Lipo-20[113] was rationally designed to co-assemble lipopeptide Lipo-S and ciprofloxacin to form nano-antibiotic transformers (NATs). NATs could specifically bind to negatively charged lipids in bacterial cell membranes and further converted into *in situ* nanofibers, thereby enhancing membrane disruption and enabling efficient intracellular delivery of ciprofloxacin. In addition, the transformed nanofiber could imitate NETs to trap bacteria. Such multiple antibacterial mechanisms of *in situ* peptide assemblies show great potential to overcome antibiotic resistance.

5. Conclusion and outlook

In recent years, *in situ* peptide assemblies have attracted increasing attention for bacterial diagnostic and therapeutic applications (Table 1). With rational design, *in situ* peptide assemblies not only have smart biomarker-activatable imaging/antibacterial properties, but also show enhanced accumulation and retention at bacterial infection sites. As such, enhanced bacterial imaging and treatment outcomes can be easily obtained by using these supramolecular assemblies. Despite the rapid advancements, several problems still need to be addressed. First, it remains a big challenge to develop *in situ* peptide assemblies with more precise spatiotemporal controllability within bacteria. Recent efforts have led to *in situ* peptide assemblies instantly targeting subcellular organelles in cancer cells.[114–119] The above successes may provide valuable guidance for the design of peptide assemblies with precise bacterial substructure-targeting capabilities. Nevertheless, bacteria are much smaller than mammalian cells and have different cellular structures, which should be taken into account when designing peptide precursor molecules. Machine learning will be a powerful tool to accelerate the prediction and discovery of ideal antimicrobial peptide precursor (or monomer) candidates.[120–122] Second, it is necessary to develop valuable tools to reveal the dynamic process of peptide assemblies in living bacteria. A deeper understanding of this fundamental question can provide rich resources for the development of *in situ* antimicrobial peptide assemblies. Third, it would be valuable to develop *in situ* peptide assemblies with other clinical imaging modalities (*e.g.*, positron emission tomography (PET), single photon emission computed tomography (SPECT), nanocomputed tomography (nano-CT)) or other antibacterial mechanisms. Additionally, more attention should be paid to the pharmacokinetics and biosafety of peptide assemblies, which may help advance their clinical translation. We believe these *in situ* peptide assemblies can provide powerful alternatives for the diagnosis and treatment of bacterial infections.

Author contributions

Y. Zhou and L. Xu contributed equally to this work. Y. Zhou, L. Xu, X. Sun, and W. Zhan contributed to the conceptualization and writing – original draft. W. Zhan and G. Liang contributed to supervision, funding acquisition, and writing – review & editing.

Conflicts of interest

The authors declare no conflict of interest.

Acknowledgements

This work was supported by the National Natural Science Foundation of China (Grants 52103158, 22234002, and 22074016).

References

1 G. B. D. Antimicrobial Resistance Collaborators, *Lancet*, 2022, **400**, 2221–2248.
2 M. F. Chellat, L. Raguz and R. Riedl, *Angew. Chem., Int. Ed.*, 2016, **55**, 6600–6626.
3 E. M. Darby, E. Trampari, P. Siasat, M. S. Gaya, I. Alav, M. A. Webber and J. M. A. Blair, *Nat. Rev. Microbiol.*, 2023, **21**, 280–295.
4 R. C. MacLean and A. San Millan, *Science*, 2019, **365**, 1082–1083.
5 L. B. Rice, *J. Infect. Dis.*, 2008, **197**, 1079–1081.

6 E. Tacconelli, E. Carrara, A. Savoldi, S. Harbarth, M. Mendelson, D. L. Monnet, C. Pulcini, G. Kahlmeter, J. Kluytmans, Y. Carmeli, M. Ouellette, K. Outterson, J. Patel, M. Cavaleri, E. M. Cox, C. R. Houchens, M. L. Grayson, P. Hansen, N. Singh, U. Theuretzbacher, N. Magrini and WHO Pathogens Priority List Working Group, *Lancet Infect. Dis.*, 2018, **18**, 318–327.
7 M.-H. Xiong, Y. Bao, X.-Z. Yang, Y.-H. Zhu and J. Wang, *Adv. Drug Delivery Rev.*, 2014, **78**, 63–76.
8 U. Theuretzbacher, S. Gottwalt, P. Beyer, M. Butler, L. Czaplewski, C. Lienhardt, L. Moja, M. Paul, S. Paulin, J. H. Rex, L. L. Silver, M. Spigelman, G. E. Thwaites, J. P. Paccaud and S. Harbarth, *Lancet Infect. Dis.*, 2019, **19**, E40–E50.
9 M. Baym, L. K. Stone and R. Kishony, *Science*, 2016, **351**, aad3292.
10 S. E. Rossiter, M. H. Fletcher and W. M. Wuest, *Chem. Rev.*, 2017, **117**, 12415–12474.
11 X. Ding, S. Duan, X. Ding, R. Liu and F.-J. Xu, *Adv. Funct. Mater.*, 2018, **28**, 1802140.
12 A. Luther, M. Urfer, M. Zahn, M. Mueller, S.-Y. Wang, M. Mondal, A. Vitale, J.-B. Hartmann, T. Sharpe, F. Lo Monte, H. Kocherla, E. Cline, G. Pessi, P. Rath, S. M. Modaresi, P. Chiquet, S. Stiegeler, C. Verbree, T. Remus, M. Schmitt, C. Kolopp, M.-A. Westwood, N. Desjonqueres, E. Brabet, S. Hell, K. LePoupon, A. Vermeulen, R. Jaisson, V. Rithie, G. Upert, A. Lederer, P. Zbinden, A. Wach, K. Moehle, K. Zerbe, H. H. Locher, F. Bernardini, G. E. Dale, L. Eberl, B. Wollscheid, S. Hiller, J. A. Robinson and D. Obrecht, *Nature*, 2019, **576**, 452–458.
13 X. Li, H. Bai, Y. Yang, J. Yoon, S. Wang and X. Zhang, *Adv. Mater.*, 2019, **31**, 1805092.
14 M. J. Mitcheltree, A. Pisipati, E. A. Syroegin, K. J. Silvestre, D. Klepacki, J. D. Mason, D. W. Terwilliger, G. Testolin, A. R. Pote, K. J. Y. Wu, R. P. Ladley, K. Chatman, A. S. Mankin, Y. S. Polikanov and A. G. Myers, *Nature*, 2021, **599**, 507–512.
15 Z. Wang, B. Koirala, Y. Hernandez, M. Zimmerman and S. F. Brady, *Science*, 2022, **376**, 991–996.
16 P. J. Weldick, A. Wang, A. F. Halbus and V. N. Paunov, *Nanoscale*, 2022, **14**, 4018–4041.
17 M. Xie, M. Gao, Y. Yun, M. Malmsten, V. M. M. Rotello, R. Zboril, O. Akhavan, A. Kraskouski, J. Amalraj, X. Cai, J. Lu, H. Zheng and R. Li, *Angew. Chem., Int. Ed.*, 2023, **62**, e202217345.
18 S. Cheeseman, A. J. Christofferson, R. Kariuki, D. Cozzolino, T. Daeneke, R. J. Crawford, V. K. Truong, J. Chapman and A. Elbourne, *Adv. Sci.*, 2020, **7**, 201902913.
19 P. Makvandi, C.-y. Wang, E. N. Zare, A. Borzacchiello, L.-n. Niu and F. R. Tay, *Adv. Funct. Mater.*, 2020, **30**, 1910021.
20 X. Zhao, H. Tang and X. Jiang, *ACS Nano*, 2022, **16**, 10066–10087.
21 Q. Xin, H. Shah, A. Nawaz, W. Xie, M. Z. Akram, A. Batool, L. Tian, S. U. Jan, R. Boddula, B. Guo, Q. Liu and J. R. Gong, *Adv. Mater.*, 2019, **31**, 201804838.
22 N. Kumar, P. Chamoli, M. Misra, M. K. Manoj and A. Sharma, *Nanoscale*, 2022, **14**, 3987–4017.
23 Y. Xue, Z. Zhao, Y. Zhao, C. Wang, S. Shen, Z. Qiu, R. Cui, S. Zhou, L. Fang, Z. Chen, H. Zhu and B. Zhu, *Nanoscale*, 2022, **14**, 12789–12803.
24 Y. Wu, K. Chen, J. Wang, M. Chen, Y. Chen, Y. She, Z. Yan and R. Liu, *Prog. Polym. Sci.*, 2023, **141**, 101679.
25 N. Kandoth, S. Barman, A. Chatterjee, S. Sarkar, A. K. Dey, S. K. Pramanik and A. Das, *Adv. Funct. Mater.*, 2021, **31**, 2104480.
26 X. Liu, Q. Zhang, W. Knoll, B. Liedberg and Y. Wang, *Adv. Mater.*, 2020, **32**, 2000866.
27 N. Liu, Y. Wang, Z. Wang, Q. He, Y. Liu, X. Dou, Z. Yin, Y. Li, H. Zhu and X. Yuan, *Nanoscale*, 2022, **14**, 8183–8191.
28 L.-L. Li, H.-W. An, B. Peng, R. Zheng and H. Wang, *Mater. Horiz.*, 2019, **6**, 1794–1811.
29 C. Ren, Z. Wang, Q. Wang, C. Yang and J. Liu, *Small Methods*, 2020, **4**, 201900403.
30 B. H. Gan, J. Gaynord, S. M. Rowe, T. Deingruber and D. R. Spring, *Chem. Soc. Rev.*, 2021, **50**, 7820–7880.
31 Y. Jiang, Y. Chen, Z. Song, Z. Tan and J. Cheng, *Adv. Drug Delivery Rev.*, 2021, **170**, 261–280.
32 P. Tan, H. Fu and X. Ma, *Nano Today*, 2021, **39**, 101229.
33 G. Li, Z. Lai and A. Shan, *Adv. Sci.*, 2023, **10**, 202206602.
34 P. Zou, W.-T. Chen, T. Sun, Y. Gao, L.-L. Li and H. Wang, *Biomater. Sci.*, 2020, **8**, 4975–4996.
35 M. Abbas, M. Ovais, A. Atiq, T. M. Ansari, R. Xing, E. Spruijt and X. Yan, *Coord. Chem. Rev.*, 2022, **460**, 214481.
36 S. Zhang, *Protein Sci.*, 2020, **29**, 2281–2303.
37 A. Levin, T. A. Hakala, L. Schnaider, G. J. L. Bernardes, E. Gazit and T. P. J. Knowles, *Nat. Rev. Chem.*, 2020, **4**, 615–634.
38 J. Zhang, Y. Wang, B. J. Rodriguez, R. Yang, Y. Bin, D. Mei, J. Li, K. Tao and E. Gazit, *Chem. Soc. Rev.*, 2022, **51**, 6936–6947.
39 Z. Liu, J. Guo, Y. Qiao and B. Xu, *Acc. Chem. Res.*, 2023, **56**, 3076–3088.
40 S. Fleming and R. V. Ulijn, *Chem. Soc. Rev.*, 2014, **43**, 8150–8177.
41 R. Chang, L. Zhao, R. Xing, J. Li and X. Yan, *Chem. Soc. Rev.*, 2023, **52**, 2688–2712.
42 T. Wang, C. Menard-Moyon and A. Bianco, *Chem. Soc. Rev.*, 2022, **51**, 3535–3560.
43 C. Vicente-Garcia and I. Colomer, *Nat. Rev. Chem.*, 2023, **7**, 710–731.
44 A. R. Mazo, S. Allison-Logan, F. Karimi, N. J.-A. Chan, W. Qiu, W. Duan, N. M. O'Brien-Simpson and G. G. Qiao, *Chem. Soc. Rev.*, 2020, **49**, 4737–4834.
45 F. Sheehan, D. Sementa, A. Jain, M. Kumar, M. Tayarani-Najjaran, D. Kroiss and R. V. Ulijn, *Chem. Rev.*, 2021, **121**, 13869–13914.

46 J. Gao, J. Zhan and Z. Yang, *Adv. Mater.*, 2020, **32**, 201805798.
47 H. He, W. Tan, J. Guo, M. Yi, A. N. Shy and B. Xu, *Chem. Rev.*, 2020, **120**, 9994–10078.
48 J. Kim, S. Lee, Y. Kim, M. Choi, I. Lee, E. Kim, C. G. Yoon, K. Pu, H. Kang and J. S. Kim, *Nat. Rev. Mater.*, 2023, **8**, 710–725.
49 S. Chagri, D. Y. W. Ng and T. Weil, *Nat. Rev. Chem.*, 2022, **6**, 320–338.
50 M. Mamuti, R. Zheng, H.-W. An and H. Wang, *Nano Today*, 2021, **36**, 101036.
51 Y. Deng, W. Zhan and G. Liang, *Adv. Healthcare Mater.*, 2021, **10**, 2001211.
52 Q. Jiang, X. Liu, G. Liang and X. Sun, *Nanoscale*, 2021, **13**, 15142–15150.
53 T. Wei, Q. Yu and H. Chen, *Adv. Healthcare Mater.*, 2019, **8**, 1801381.
54 Z. Wang, X. Liu, Y. Duan and Y. Huang, *Biomaterials*, 2022, **280**, 121249.
55 Z. Yang, G. Liang, Z. Guo, Z. Guo and B. Xu, *Angew. Chem., Int. Ed.*, 2007, **46**, 8216–8219.
56 W. Zhan, L. Xu, Z. Liu, X. Liu, G. Gao, T. Xia, X. Cheng, X. Sun, F. G. Wu, Q. Yu and G. Liang, *Angew. Chem., Int. Ed.*, 2023, **62**, e202306427.
57 V. K. Pal and S. Roy, *ACS Appl. Nano Mater.*, 2022, **5**, 12019–12034.
58 T. Li, C. Zhu, C. Liang, T. Deng, X. Wu, K. Wen, X. Feng, D. Yuan, B. Xu and J. Shi, *ACS Appl. Nano Mater.*, 2023, **6**, 7785–7793.
59 J.-C. Lagier, S. Edouard, I. Pagnier, O. Mediannikov, M. Drancourt and D. Raoult, *Clin. Microbiol. Rev.*, 2015, **28**, 208–236.
60 C. Deusenbery, Y. Wang and A. Shukla, *ACS Infect. Dis.*, 2021, **7**, 695–720.
61 Z. Wang, C. Thang Do, W. Zhong, J. W. Lau, G. Kwek, M. B. Chan-Park and B. Xing, *Angew. Chem., Int. Ed.*, 2021, **60**, 16900–16905.
62 L. Xu, W. Zhan, Y. Deng, X. Liu, G. Gao, X. Sun and G. Liang, *Adv. Healthcare Mater.*, 2022, **11**, 2200453.
63 Y. Zhang, M. Hao, L. Li, Q. Luo, S. Deng, Y. Yang, Y. Liu, W. Fang and E. Song, *TrAC, Trends Anal. Chem.*, 2023, **159**, 116916.
64 Y. Huang, W. Chen, J. Chung, J. Yin and J. Yoon, *Chem. Soc. Rev.*, 2021, **50**, 7725–7744.
65 C. Yang, C. Ren, J. Zhou, J. Liu, Y. Zhang, F. Huang, D. Ding, B. Xu and J. Liu, *Angew. Chem., Int. Ed.*, 2017, **56**, 2356–2360.
66 Y. Hong, J. W. Y. Lam and B. Z. Tang, *Chem. Soc. Rev.*, 2011, **40**, 5361–5388.
67 D. Ding, K. Li, B. Liu and B. Z. Tang, *Acc. Chem. Res.*, 2013, **46**, 2441–2453.
68 G. Qi, F. Hu, L. S. Kenry, L. Shi, M. Wu and B. Liu, *Angew. Chem., Int. Ed.*, 2019, **58**, 16229–16235.
69 X. Zhang, C. Ren, F. Hu, Y. Gao, Z. Wang, H. Li, J. Liu, B. Liu and C. Yang, *Anal. Chem.*, 2020, **92**, 5185–5190.
70 L. Zhang, Y. Li, G. Mu, L. Yang, C. Ren, Z. Wang, Q. Guo, J. Liu and C. Yang, *Anal. Chem.*, 2022, **94**, 2236–2243.
71 Y. Liu, L. Teng, B. Yin, H. Meng, X. Yin, S. Huan, G. Song and X.-B. Zhang, *Chem. Rev.*, 2022, **122**, 6850–6918.
72 L. Lin and L. V. Wang, *Nat. Rev. Clin. Oncol.*, 2022, **19**, 365–384.
73 W. Choi, B. Park, S. Choi, D. Oh, J. Kim and C. Kim, *Chem. Rev.*, 2023, **123**, 7379–7419.
74 H. Zhu, B. Li, C. Y. Chan, B. L. Q. Ling, J. Tor, X. Y. Oh, W. Jiang, E. Ye, Z. Li and X. J. Loh, *Adv. Drug Delivery Rev.*, 2023, **192**, 114644.
75 H.-B. Cheng, Y. Li, B. Z. Tang and J. Yoon, *Chem. Soc. Rev.*, 2020, **49**, 21–31.
76 K. Pu, A. J. Shuhendler, J. V. Jokerst, J. Mei, S. S. Gambhir, Z. Bao and J. Rao, *Nat. Nanotechnol.*, 2014, **9**, 233–239.
77 Q. Cai, Y. Fei, L. Hu, Z. Huang, L.-L. Li and H. Wang, *Nano Lett.*, 2018, **18**, 6229–6236.
78 L.-L. Li, Q. Zeng, W.-J. Liu, X.-F. Hu, Y. Li, J. Pan, D. Wan and H. Wang, *ACS Appl. Mater. Interfaces*, 2016, **8**, 17936–17943.
79 L.-L. Li, H.-L. Ma, G.-B. Qi, D. Zhang, F. Yu, Z. Hu and H. Wang, *Adv. Mater.*, 2016, **28**, 254–262.
80 S.-Z. Lu, X.-Y. Guo, M.-S. Zou, Z.-Q. Zheng, Y.-C. Li, X.-D. Li, L.-L. Li and H. Wang, *Adv. Healthcare Mater.*, 2020, **9**, 1901229.
81 H.-D. Xu, X. Cheng, X. Sun, P. Chen, W. Zhan, X. Liu, X. Wang, B. Hu and G. Liang, *Nano Lett.*, 2023, **23**, 6178–6183.
82 Y. Li, X. Hu, D. Ding, Y. Zou, Y. Xu, X. Wang, Y. Zhang, L. Chen, Z. Chen and W. Tan, *Nat. Commun.*, 2017, **8**, 15653.
83 Z. Hai, Y. Ni, D. Saimi, H. Yang, H. Tong, K. Zhong and G. Liang, *Nano Lett.*, 2019, **19**, 2428–2433.
84 L. Li, P. Gu, M. Hao, X. Xiang, Y. Feng, X. Zhu, Y. Song and E. Song, *Small*, 2021, **17**, 2103627.
85 D. Wang, D.-B. Cheng, L. Ji, L.-J. Niu, X.-H. Zhang, Y. Cong, R.-H. Cao, L. Zhou, F. Bai, Z.-Y. Qiao and H. Wang, *Biomaterials*, 2021, **264**, 120386.
86 L. Li, M. Liu, S. Deng, X. Zhu, Y. Song and E. Song, *Small*, 2023, **19**, 202208249.
87 L. Li, M. Liu, S. Deng, X. Zhu, Y. Song and E. Song, *Acta Biomater.*, 2023, **164**, 487–495.
88 H. Wang, Z. Feng and B. Xu, *Angew. Chem., Int. Ed.*, 2019, **58**, 10423–10432.
89 R. A. Pires, Y. M. Abul-Haija, D. S. Costa, R. Novoa-Carballal, R. L. Reis, R. V. Ulijn and I. Pashkuleva, *J. Am. Chem. Soc.*, 2015, **137**, 576–579.
90 W. Gao, Y. Chen, Y. Zhang, Q. Zhang and L. Zhang, *Adv. Drug Delivery Rev.*, 2018, **127**, 46–57.
91 C. K. C. Lai, R. W. Y. Ng, S. S. Y. Leung, M. Hui and M. Ip, *Adv. Drug Delivery Rev.*, 2022, **181**, 114078.
92 F. Zhang, J. Zhuang, Z. Li, H. Gong, B. E.-F. de Avila, Y. Duan, Q. Zhang, J. Zhou, L. Yin, E. Karshalev, W. Gao, V. Nizet, R. H. Fang, L. Zhang and J. Wang, *Nat. Mater.*, 2022, **21**, 1324–1332.

93 C. Yang, F. Hu, X. Zhang, C. Ren, F. Huang, J. Liu, Y. Zhang, L. Yang, Y. Gao, B. Liu and J. Liu, *Biomaterials*, 2020, **244**, 119972.
94 X. Cheng, X. Pei, W. Xie, J. Chen, Y. Li, J. Wang, H. Gao and Q. Wan, *Small*, 2022, **18**, 2200915.
95 Y. Wang, Y. Yang, Y. Shi, H. Song and C. Yu, *Adv. Mater.*, 2020, **32**, 201904106.
96 P. P. Kalelkar, M. Riddick and A. J. Garcia, *Nat. Rev. Mater.*, 2022, **7**, 39–54.
97 G.-B. Qi, D. Zhang, F.-H. Liu, Z.-Y. Qiao and H. Wang, *Adv. Mater.*, 2017, **29**, 1703461.
98 X.-Y. Zhang, C. Liu, P.-S. Fan, X.-H. Zhang, D.-Y. Hou, J.-Q. Wang, H. Yang, H. Wang and Z.-Y. Qiao, *J. Mater. Chem. B*, 2022, **10**, 3624–3636.
99 R. Teng, Y. Yang, Z. Zhang, K. Yang, M. Sun, C. Li, Z. Fan and J. Du, *Adv. Funct. Mater.*, 2023, **33**, 2214454.
100 Z. Gong, Y. Shi, H. Tan, L. Wang, Z. Gao, B. Lian, G. Wang, H. Sun, P. Sun, B. Zhou and J. Bair, *ACS Appl. Mater. Interfaces*, 2020, **12**, 4323–4332.
101 Q.-H. Yu, R. Huang, K.-Y. Wu, X.-L. Han, Y.-J. Cheng, W.-L. Liu, A.-Q. Zhang and S.-Y. Qin, *Acta Biomater.*, 2022, **154**, 359–373.
102 P. Tan, C. Wu, Q. Tang, T. Wang, C. Zhou, Y. Ding, H. Fu, S. Xu, Y. Feng, Y. Zhang, Q. Dai and X. Ma, *Adv. Mater.*, 2023, **35**, 2210766.
103 Z. Shen, Z. Guo, L. Zhou, Y. Wang, J. Zhang, J. Hu and Y. Zhang, *Biomater. Sci.*, 2020, **8**, 2031–2039.
104 D. Zhang, J. Liu, Q. Chen, W. Jiang, Y. Wang, J. Xie, K. Ma, C. Shi, H. Zhang, M. Chen, J. Wan, P. Ma, J. Zou, W. Zhang, F. Zhou and R. Liu, *Nat. Commun.*, 2021, **12**, 6331.
105 Y. Li, L. Su, Y. Zhang, Y. Liu, F. Huang, Y. Ren, Y. An, L. Shi, H. C. van der Mei and H. J. Busscher, *Adv. Sci.*, 2022, **9**, 202103485.
106 L. Chen, M. Peng, J. Zhou, X. Hu, Y. Piao, H. Li, R. Hu, Y. Li, L. Shi and Y. Liu, *Adv. Mater.*, 2023, **35**, 202301664.
107 W. Zhan, G. Gao, Z. Liu, X. Liu, L. Xu, M. Wang, H.-D. Xu, R. Tang, J. Cao, X. Sun and G. Liang, *Adv. Healthcare Mater.*, 2023, **12**, 2203283.
108 P. Chairatana and E. M. Nolan, *Acc. Chem. Res.*, 2017, **50**, 960–967.
109 Y. Fan, X.-D. Li, P.-P. He, X.-X. Hu, K. Zhang, J.-Q. Fan, P.-P. Yang, H.-Y. Zheng, W. Tian, Z.-M. Chen, L. Ji, H. Wang and L. Wang, *Sci. Adv.*, 2020, **6**, eaaz4767.
110 Z. Huang, Y. Liu, L. Wang, A. Ali, Q. Yao, X. Jiang and Y. Gao, *Biomaterials*, 2020, **253**, 120124.
111 J. Chen, P. Zhang, Y. Zhao, J. Zhao, X. Wu, R. Zhang, R. Cha, Q. Yao and Y. Gao, *Sci. Adv.*, 2022, **8**, eadd2789.
112 J. Liu, X. Zhang, P. Zou, J. Yao, L. Liu, Y. Cai, T. Sun, Y. Gao and L.-L. Li, *Nano Today*, 2022, **44**, 101505.
113 P. Zou, J. Liu, X. Li, M. Yaseen, J. Yao, L. Liu, L. Luo, H. Wang, X. Shi, Z. Li, T. Sun, Y. Gao, C. Gao and L.-L. Li, *ACS Nano*, 2022, **16**, 20545–20558.
114 S. Liu, Q. Zhang, H. He, M. Yi, W. Tan, J. Guo and B. Xu, *Angew. Chem., Int. Ed.*, 2022, **61**, e202210568.
115 W. Tan, Q. Zhang, M. C. Quiñones-Frías, A. Y. Hsu, Y. Zhang, A. Rodal, P. Hong, H. R. Luo and B. Xu, *J. Am. Chem. Soc.*, 2022, **144**, 6709–6713.
116 J. Wang, L. Hu, H. Zhang, Y. Fang, T. Wang and H. Wang, *Adv. Mater.*, 2022, **34**, 2104704.
117 B. Jana, S. Jin, E. M. Go, Y. Cho, D. Kim, S. Kim, S. K. Kwak and J.-H. Ryu, *J. Am. Chem. Soc.*, 2023, **145**, 18414–18431.
118 S. Kim, H. Choi, S. Jin, S. Son, Y. Lee, K. Kim and J.-H. Ryu, *Giant*, 2023, **16**, 100189.
119 X. Liu, W. Zhan, G. Gao, Q. Jiang, X. Zhang, H. Zhang, X. Sun, W. Han, F.-G. Wu and G. Liang, *J. Am. Chem. Soc.*, 2023, **145**, 7918–7930.
120 R. Batra, T. D. Loeffler, H. Chan, S. Srinivasan, H. Cui, I. V. Korendovych, V. Nanda, L. C. Palmer, L. A. Solomon, H. C. Fry and S. K. R. S. Sankaranarayanan, *Nat. Chem.*, 2022, **14**, 1427–1435.
121 M. Ramakrishnan, A. van Teijlingen, T. Tuttle and R. V. Ulijn, *Angew. Chem., Int. Ed.*, 2023, **62**, 202218067.
122 T. Xu, J. Wang, S. Zhao, D. Chen, H. Zhang, Y. Fang, N. Kong, Z. Zhou, W. Li and H. Wang, *Nat. Commun.*, 2023, **14**, 3880.